



# A low cost smart power meter for IoT

F. Abate<sup>c</sup>, M. Carratù<sup>a,\*</sup>, C. Liguori<sup>a</sup>, V. Paciello<sup>b</sup>

<sup>a</sup> Dept. of Industrial Engineering, University of Salerno, Via Giovanni Paolo II, 132 Fisciano, SA, Italy

<sup>b</sup> Dept. of Electrical Engineering and Information, University of Cassino and Southern Lazio, Via G. Di Biasio, 43 Cassino, FR, Italy

<sup>c</sup> R&D, Spring off s.r.l., Via Tenente Nastri, 153 Fisciano, SA, Italy

## ARTICLE INFO

### Article history:

Received 31 July 2018

Received in revised form 16 December 2018

Accepted 21 December 2018

Available online 23 December 2018

### Keywords:

Smart city

Smart grid

Smart meter

AMI

Demand side management

Open metering

IoT

## ABSTRACT

The smart city in urban planning and architecture is a set of urban planning strategies aimed at optimizing and innovating public services so as to relate the material infrastructures of cities “with the human, intellectual and social capital of those who live there” thanks to the widespread use of new communication technologies, mobility, environment and energy efficiency, in order to improve the quality of life and meet the needs of citizens, businesses and institutions. Nowadays we hear more and more about the Internet of Things (IoT). Smart devices connected to the internet are increasing in cities. Cities become smart, but at the same time it is not considered the quality of data that these devices send over the internet. The authors, starting from the experience gained previously, in this work focus on energy efficiency, and in particular how energy measurements are performed and sent. The authors propose a low cost smart electric meter for the measurement of electrical parameters. The meter is capable of adapting to the variability of the grid maintaining a high level of measurement accuracy. On the proposed smart meter two algorithms are developed and compared both in simulation and with real signals.

© 2018 Elsevier Ltd. All rights reserved.

## 1. Introduction

Nowadays, the concept of the Internet of Things (IoT) is increasingly stated as the environment of interconnected people and object among themselves: it is not just about machine to machine communication (M2M), the IoT is about the way humans and machines connect, using common public services.

This kind of network is composed by smart devices: stand-alone devices able to monitor or interact with their surroundings. Furthermore, with the term “smart” is mean that these things are able to acquire data from the environment, process and communicate them to other objects, and to interact autonomously with the environment relying on data exploiting the embedded electronics, software sensors, actuators and communication capabilities.

More in details, these sets of smart objects, distributed in the environment and combined in different contexts, could substantially improve the way people interacts with their surroundings, creating services and application in any branch. In particular, IoT devices are the means through the Smart Cities [1–5]. The concept of an intelligent city is a strategic feature for modern society because it provides to citizens Information and Communication Technologies (ICT) services driven by real data, and makes the cit-

izens themselves became a central and active part of the city, interacting in a bidirectional way with these services. New business models based on real-time pricing or active load control could be introduced thanks to the implementation of a network of measuring devices, enabling the end-user to get better tariffs [6]. Therefore, the quality of services offered by a Smart City critically depends on the Smart Things used, as well as the ability to make citizens aware of the use of these new technologies.

The main facilities offered by a smart city could be resumed in three main group: Smart Building, Smart Health and Smart Grid (Fig. 1).

More in details, the Smart Buildings offer the possibility to share and analyse data that could be used to control and improve the building management systems using pervasive wireless connectivity, sensors and IoT technologies. Different IoT solutions are used in order to automate security systems, access control, lighting, HVAC (Heating, Ventilation and Air Conditioning) systems, etc. Moreover, a Smart Building offer greater efficiency, safety and comfort, while providing a cost savings for the property owners, managers and tenants.

On the other hand, the Smart Healthcare deals with the development of technologies that lead to better treatment for patients, better and widespread diagnostic tools, and devices that improve the quality of life for anyone connected to the IoT world.

Probably, the facility behind all the smart cities innovations is represented by the Smart Grid. The smart grid represents an

\* Corresponding author.

E-mail address: [mcarratu@unisa.it](mailto:mcarratu@unisa.it) (M. Carratù).

URL: <http://www.misure.unisa.it> (M. Carratù).

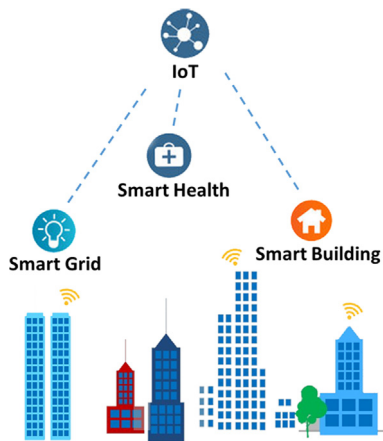


Fig. 1. Principal services of a smart city.

electrical grid, which includes many operations and energy measures. About the smart grids, due to the global demand of worldwide electricity, and the opportunity given by distributed generation and renewable sources, most of the electric grids projected and realized decades ago, are now struggling to run into the new challenges available in a smart city. In this context, studying, researching and developing of smart grids is fundamental, in order to achieve the full potential for the smart cities of the future [7].

The bi-directionality data communication will characterize the Smart Grids in order to share among all relevant users of the energy conversion chain [8,9], responsibilities and benefits [10]. Consumers, utilities, and service providers will result to be part of a participatory network.

Principally, smart grids will help the consumers with information to manage, monitor, control the energy usage, and optimize performance according to demand. Moreover, there would be benefits both for suppliers and customers: one would be able to manage the peak demand side, and the other one would be able to monitor and optimize their energy consumption related to the real-time price of energy and individual needs [11,12].

An example of common open network for smart grid devices is the Automated Metering Infrastructure (AMI) [13]: it is a standard architecture to implement a full-scale bi-directional data communication. Data collected over an AMI can be stored, captured and forwarded to a central access system.

Furthermore, the sensing elements in this interconnected scenario are the key point to monitor energy, because on these elements all the data exchanged in the grid are founded [14,15]: the device that include this communication and sensing capabilities in the power grid is the Smart Power Meter. In order to achieve a widespread dissemination of these kind of devices, it is required that they are simultaneously affordable and accurate, because they have to be capillary distributed, but they are also the acquisition point for the smart grids.

Since the introduction of nonlinear and active loads on the power grid, the active and reactive power must be measured in non-sinusoidal conditions; indeed, on the power grid we can see phenomena such as voltage sags and swells, harmonic distortion that changes harmonic distortions significantly the expected sinusoidal signal. Many metrics used for energy evaluation consider the power grid frequency constant, then many the smart power meters on the market make an error in the energy evaluation [16–18]. Also, in the literature the problem remains unconsidered: there are different papers that consider constant the power grid frequency in the evaluation of energy consumption [19–21].

In this paper, a low-cost device is proposed, that is able to measure energy in a sufficient accurate way. On the proposed architec-

ture two algorithms were compared, which allow to obtain a better measure of the power grid frequency, without complicate the hardware requirements. Starting from previous works in the fields of remote metering and wireless sensor networks [22–25], the authors propose to evaluate the performance of a low-cost smart power meter based on a common chip.

## 2. The IoT network infrastructure

### 2.1. Overview

Speaking of Smart Objects, it is very important to consider the nature of the network that interconnects them. The network infrastructure has the task of making the various nodes of the network reachable. The main objectives of a communication infrastructure are represented by the possibility of access to the data for users and developers and the reachability of the node not intended solely to the data relating to it. Another important parameter concerning network infrastructures regards their degree of maturity, indeed, the use of consolidated infrastructures allows for technological solutions available on the market. In the IoT field, the network infrastructure is mainly short-range, which are now widely used for the mobile reading of main meters that are particularly difficult to read and for the remote reading of domestic divisional meters, identifying small networks privately managed. An example is given by the continuous growth of the accounting water and heat market where meters can be read through mobile or fixed systems, quickly and economically, bringing numerous benefits to users. The generic term Low-Power Wide-Area Network (LPWAN) identifies a group of technologies that perfectly meet the needs of the IoT. The main features of the LPWAN are represented by low consumption since the end-points are often powered by batteries that must provide energy for 10 years and long transmission range with good penetration characteristics for complex installations. The reduction of the complexity and cost of the network infrastructure it is also fundamental to obtain a low cost per end-point. The LPWAN solutions are designed precisely to meet these needs, drastically reducing the cost of the infrastructure and allowing to connect to the same network many other devices and sensors in addition to gas and water meters already present into the smart city [26].

LPWAN solutions such as wM-Bus, LoRa™, Sigfox and NB-IoT allow long-range connectivity and have a lower infrastructure cost to connect different types of sensors (IoT), in different types of applications, such as smart metering, smart building and smart health, which can bring more value and savings compared to dedicated solutions as GPRS or 3G. The target of these technologies are the applications that must transmit little data, which require low cost of connectivity and that must be powered by batteries for a long time. Cellular connectivity through existing networks already allows similar performance, but generally at a higher cost for each end-point.

The LPWAN solutions previously reported use free frequencies (ISM unlicensed spectrum) at 868 (Europe), 169 (Europe) and 915 (USA) MHz. In order to exploit the existing wM-Bus network infrastructure at 169 MHz for remote reading of gas and water meters, the proposed smart power meter has been developed, including a radio module compatible with this IoT network infrastructure.

### 2.2. The wM-Bus short range network

The wM-Bus standard specifies the communication protocol between low-cost, batteries operated meters and a stationary data

concentrator or a mobile reader. Fig. 2 shows the wM-Bus frame used in this work, more in details:

- The L-field indicates the length of the entire message.
- The C-field indicates the type of message (request, send, response expected, ACK).
- The Sender Address represents the address of the sending device and it is composed by the concatenation of an identification number (4 bytes), a version code (1 byte) and a device type code (1 byte).
- The CRC-field contains the Cyclic Redundancy Check.
- The Data-Field contains a maximum of 120 bytes left free to the developer and used in this work as reported in Fig. 2.
- The CI-field represents the Control Information in order to indicate the protocol used in the Data-Field to the upper layer.

More specifically, the data field of the wM-Bus follows the DLMS-COSEM specification for data modelling, which is the common language for AMI technologies [27]. The wM-Bus transceivers require low energy thanks to a low-overhead protocol, transmission-only modes (which do not require an idle receive phase) and long-range sub-GHz transmission bands (see Fig. 3). In these bidirectional communication modes, the meter starts the transmission to the concentrator, being the latter always in reception.

### 2.3. Power meter prototype

The prototype unit described in [24] has been now completed with a suitable radio module, which makes the electrical power meter be a wM-Bus Repeater (according to the standard EN 13757-5:2011). This means that the electrical power meter is able to collect also measurement data received from the water and gas meter and other end-points, thus extending the transmission range of the RF network. To achieve a capillary distribution, smart power meter has to meet many different requirements: low cost, high accuracy in measuring energy consumptions, communication capabilities, and so on. Focusing these aspects and following the “Active Electrical Energy Meter” [36], a prototype of the smart power meter has been realized, ensuring the bidirectional communication channels required for an AMI scenario by means of a single-chip radio transceiver wM-BUS device. The prototype is composed by two PCB, one for acquisition and the other for elaboration and communication tasks. In Fig. 4 is reported the realized prototype, and it is showed the main chip ADE7913 on which is based the smart power meter, the dimensions of this PCB are 5 cm length and 3 cm width.

ADE7913 chip has an isolated and integrated DC/DC power converter and three second-order sigma-delta analog-digital convert-

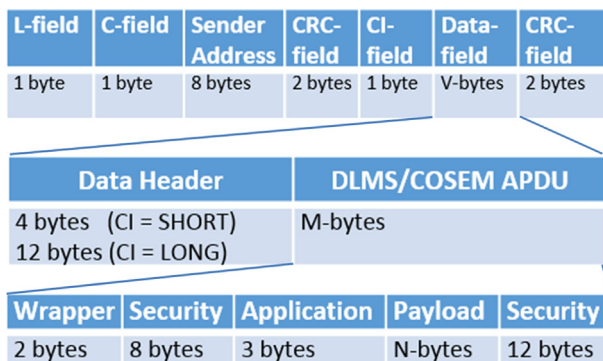


Fig. 2. The frame of the wM-Bus.

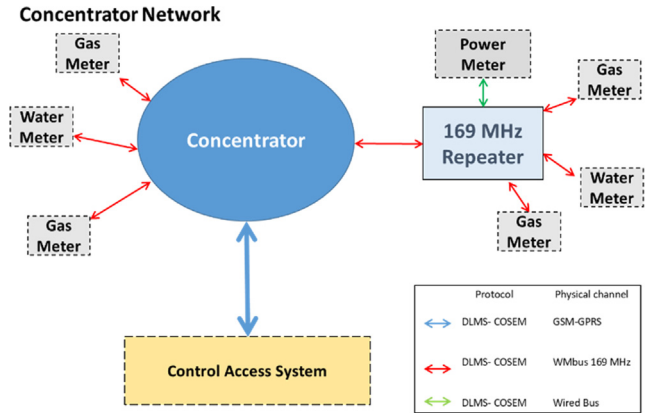


Fig. 3. Concentrator network.

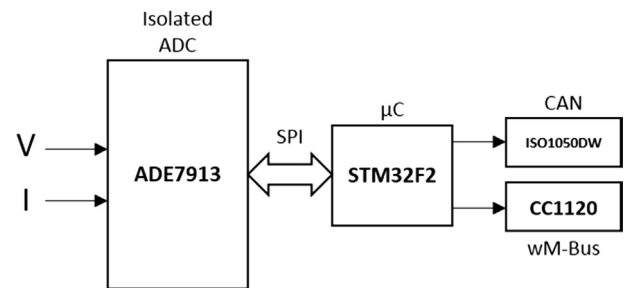


Fig. 4. The realized prototype of smart meter.

ers with a sampling rate set at 1024 MHz, 24-bit and output data rate of 1 kHz. This device communicates with an SPI interface data acquired with a microcontroller. The dimensions of this second PCB are 9 cm length and 5 cm width. Based on previous experience [22], the authors chosen, instead of use voltage and current transducers, to use a  $\Sigma$ - $\Delta$  24-bit isolated ADC converter. Moreover, another feature of this approach is the use of a shunt resistor as a sensing element for electric current, and few passive components to obtain an isolated digital output with acquired samples. These choices allow to reduce the cost for components of almost one order of magnitude: the unit price of the shunt resistor used (WSLP40261L000FEA from Vishay) is about 2 €, and the ADE7913 is around 10 €, whereas, only for the couple of transducer for voltage and current, prices are almost one hundred euros. With these components, the prototype is able to measure power up to 5 kW.

Other relevant components on the prototype are: an STM32F2 [35] microcontroller (used to acquire data, process data, calculate power, measure network frequency and energy) and, in addition to the wM-Bus interface [24,37] operating at 169 MHz, usually used in AMI scenario [38,39], a CAN bus interface.

### 2.4. Smart meter software

In literature, several algorithms have been proposed ignoring the nature of the network that must be characterized in a non-sinusoidal regime. This fact leads to an inaccurate measurement of the energy delivered.

Considering the limited resources provided by the smart power meter, in order to obtain a real-time processing, particular attention has been devoted to the selection of the appropriate measurement algorithm. The correct measurement of the grid frequency variations, due to the insertion or removal of loads with different nature during the day, must be done in order to minimize the error accounted in the power measurement. Further parameter has been

computed in order to monitor the power quality as the Total Harmonic Distortion (THD).

### 3. The choose of the power measurement metrics

#### 3.1. Power measurement in non-sinusoidal condition

The standard IEEE 1459 [30] attempts to address this topic, but up to now, there is not a unanimous agreement on the metrics (or for their correction factors) that must be used. The main idea reported in the IEEE 1459 is the decomposition of voltages and electric currents in two parts: a component representing the signal at the fundamental frequency and another component representing all the harmonics and inter-harmonics considered harmful for the electrical system. The standard relies implicitly to the use of the Fast Fourier Transform (FFT), but both time and frequency domain can be eligible for the measurement of power.

#### 3.2. The chosen metrics

The authors in this work have adopted the Fryze's approach [31] as the metric for evaluate the power quantities. In [32,33] different interpretations regarding the significance of such terms and metrics can be found. In few words, the Fryze's theory is based on the consideration that all the active power components can be defined as the power parts that cannot be considered as non-active.

One the most important motivations regarding the adoption of the Fryze's approach is to assure the real time performance of the meter, considering that the time domain approach needs less processing resource. See [28] and [31] for details on the analytical evaluation.

#### 3.3. Fundamental frequency evaluation

A fundamental aspect for the correct application of the power metrics is the definition of the observation period  $T$ : it must be an entire multiple of the fundamental period. The wanted quantities can be obtained integrating the voltage and electric current, but in a smart meter based on digital processing the integrals are calculated as a summation of the acquired samples ( $T_1$ ), this fact leads with a synchronized sampling ( $T_c$ ) in order to guarantee that the calculation is made on a multiple of fundamental period as reported in the following equation.

$$NT_c = kT_1 \quad (1)$$

For the reason previously introduced, the smart power meter should be able to measure the frequency grid variation to maintain its measurement performance. The use of a fixed sampling frequency could introduce an error in the estimation of the delivered energy due to the energy calculation depends on the network frequency. If an entire number of samples in the time interval analysis are not available, an interpolation algorithm should be used in order to avoid errors in the calculation of the power consumption. Instead of using an interpolation algorithm, an adaptive algorithm could be used to dynamically change the number of samples in the time interval analyzed.

To measure the network frequency, the authors have implemented and compared two different methods, the first one is based on the Goertzel algorithm [29] in order to estimate the spectrum near to the expected frequency, followed by an interpolation of the spectrum, and the second one based on the zero-crossing algorithm. More in details, the Goertzel algorithm has been investigated instead of other algorithms due to low computational burden achieved thanks to the calculation of only few tones of

the signal under investigation, achieving a computational complexity lower with respect to other frequency domain algorithm. Today, modern meter already implements some basic frequency measurement functions, frequently based on zero-crossing algorithm, such as the TIDM-Metrology from Texas Instruments, or the STPM series from ST Microcontroller. So, the zero-crossing algorithm has been used for the comparison since it is one of the most frequency calculation algorithm used on energy meters.

#### 3.3.1. The Goertzel algorithm

The frequency evaluation is made calculating (as explained in [18]) the module of the voltage spectrum ( $M(k)$ ) in five frequencies, ( $k$  is respectively 40, 45, 50, 55 and 60 [Hz]), centred around the expected fundamental, by means the Goertzel algorithm. These values are analyzed in order to search the maximum of the obtained lobe and find the actual frequency value. An interpolation algorithm, as reported in [23], allows measuring the frequency with a better resolution (in Fig. 5, on the left side, an algorithm extract is reported).

#### 3.3.2. The zero-crossing algorithm

This simple calculation method [34] computes the time interval of the period counting the sample points that fall into two consecutive crossing (positive or negative), considering a generic asynchronous sampling (Fig. 5, right side). The input signal frequency can be obtained adding to the counted samples the fraction of the sampling time  $\delta_1$  and  $\delta_2$ . A common approach is to apply this technique on a filtered signal, and averaging results on a specified number of measured periods. Simulations (Fig. 7) and experimental results (Table 1) of this comparison are reported in the following.

#### 3.4. Power sign determination

The power measurement in a bidirectional context as a smart grid needs to evaluate the sign of the non-active power. This

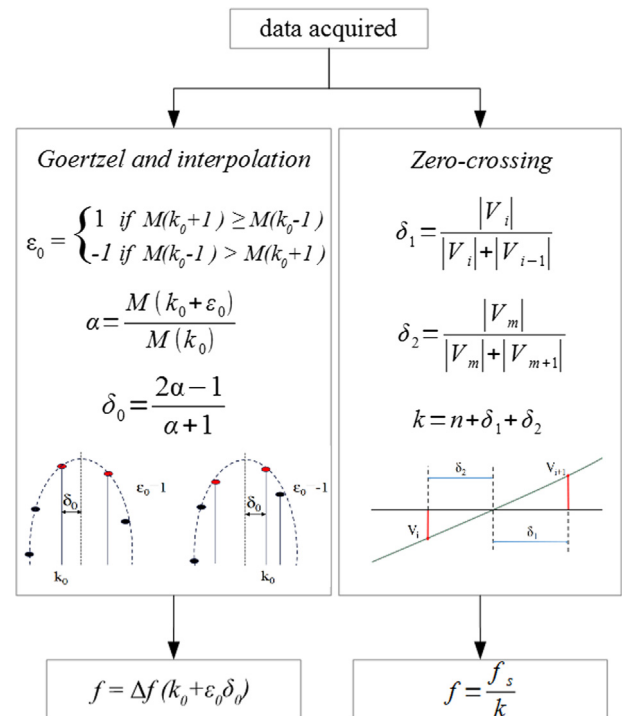


Fig. 5. Block diagram for comparison of the two algorithms implemented.



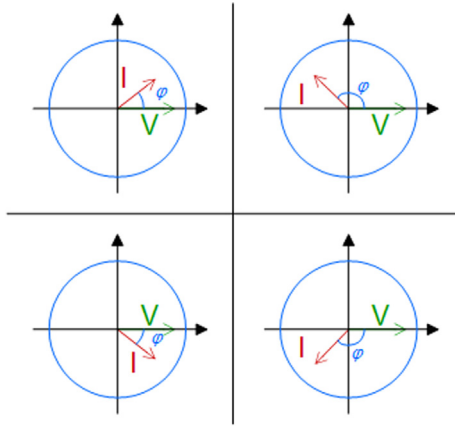


Fig. 6. Quadrants graphical representation of power flow directions.

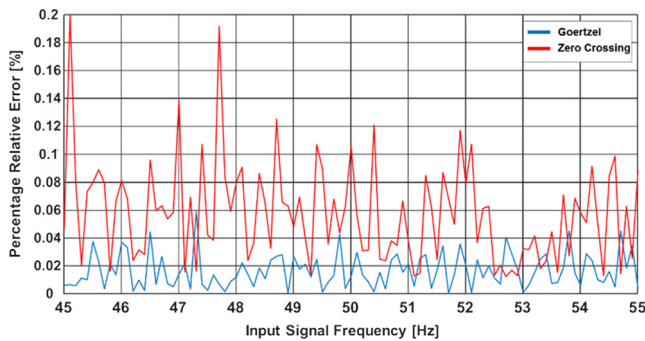


Fig. 7. Percentage relative error with Goertzel and zero-crossing techniques.

Table 1

Percentage relative error for different waveforms, referring to the calibrator frequency.

Frequency error [%]	Zero-crossing	Goertzel
Sinusoidal	6.4E-01	1.1E-03
DIP	2.9E+01	1.0E+00
Interharmonic	5.7E-01	1.2E-03
Flicker	5.1E-01	1.1E-03
Armonics Quadriform	2.0E-01	1.2E-03
Armonics Peaked	7.6E-04	1.2E-03

information about the power flow direction is given by the phase difference between the voltage and the electric current components considering the fundamental frequency. More in details, if the phase difference between voltage and electric current has a positive sign, the non-active power is positive, otherwise it is negative (see Fig. 6). For determining the voltage and electric current phases, the measured spectrum (thanks to the Goertzel algorithm) components are used.

#### 4. The simulation and experimental results

##### 4.1. Comparison between the frequency estimation algorithms

The two algorithms previously presented for the signal frequency estimation have been tested on a simulate signal using Matlab® R2017b. For the simulation, a sinusoidal signal with a  $V_{rms} = 230$  V has been generated considering  $N = 1000$  points and adding a Gaussian noise (30 dB SNR). For both the Goertzel and Zero Crossing algorithms the input frequency of the simulated sinusoidal signal has been changed between 45 Hz and 55 Hz whit

step of 0.1 Hz. The results of the simulation have been reported in Fig. 7, where the percentage relative error committed in the frequency estimation by the two-presented algorithm is shown. As predictable, the frequency estimation obtained with the approach based on the Goertzel algorithm results be better than the one obtained with the zero-crossing approach. More in details, both the approaches present a small error, but the approach based on the Goertzel algorithm has an error smaller than 0.04% versus the 0.2% obtained with the zero-crossing algorithm.

##### 4.2. Data acquisition and processing

A firmware has been implemented on the proposed smart meter. The data acquisition and processing algorithm, shown in the flowchart (Fig. 8) analyzes the quantities of interest each observation window of 200 ms, computing the voltage and electric current rms values  $V_{rms}$  and  $I_{rms}$ , the active power  $P$ , the apparent power  $S$ , the power factor  $PF$ , the module of the voltage spectrum in five frequencies, the fundamental frequency  $f_0$ , the non-active power  $N$  and its sign, and the energy  $E$ , calculated on a variable

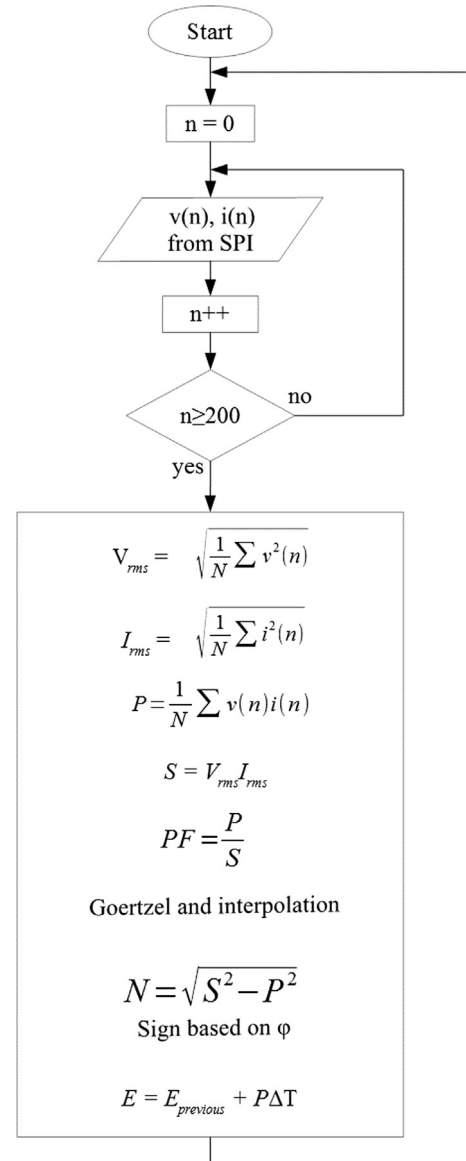


Fig. 8. Flowchart of the data acquisition and processing firmware.

number of point, correlated to the fundamental frequency which is updated every time interval analysis as reported previously. This main task is always in execution; different interrupt routines have been implemented, including the most significant based on DLMS-COSEM for data exchange.

#### 4.3. Experimental results

In this section, several experimental results are shown: these results are obtained using a set-up composed by (see Fig. 9):

- The Fluke 6105A
- The Smart Meter prototype, based on chip ADE7913.

The Fluke 6105A is a precise instrument for the calibration of Watthour meters and it proper used as an energy reference standard: it has features concerning power and energy signals traceability, and it gives a full independent control of voltage and electric current. It will supply pure sinusoidal voltage to 1 kV and current to 50 A with features such as: resolution and accuracy, less than 0.005% (50 ppm); phase performance accuracy up to 2.3 millidegrees; multi-phase operation; generation of fluctuating harmonics or inter-harmonics, voltage sags and swells, flicker, according to the IEC 61000-4 [40].

The experimental results achieved have considered also the temperature dependency of the prototype measurement module.

##### 4.3.1. Temperature calibration

The temperature calibration of the module has been carried out into a climate chamber, settling seven calibration voltages among  $-300$  V to  $300$  V and considering five temperature values ( $10^\circ\text{C}$ ,  $25^\circ\text{C}$ ,  $40^\circ\text{C}$ ,  $55^\circ\text{C}$ ,  $70^\circ\text{C}$ ). For each temperature,  $N = 1000$  samples have been considered. The relations achieved between readings, values and temperatures (see Fig. 10) have allowed to obtain a regression function for the temperature compensation of the prototype.

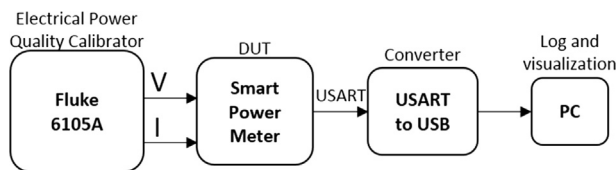


Fig. 9. Functional block diagram of experimental setup.

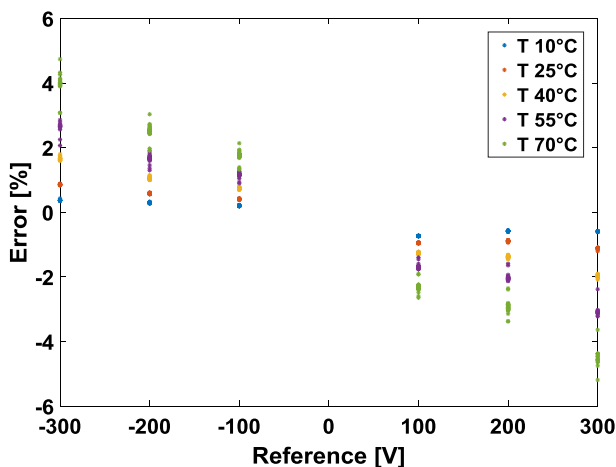


Fig. 10. Error versus voltage at different temperatures.

#### 4.3.2. Results

Firstly, the results were obtained implementing the specification of the OIML R-46 on Active Electrical Energy Meters [36]. Referring to the recommended measurements in distorted conditions, sinusoidal, DIP, Inter-harmonic, Flicker, Quadri-form and Peaked waveforms was generated using the Fluke 6105A Power Quality Calibrator. In these different conditions, the signal frequency was measured with the proposed prototype, implementing Goertzel and zero crossing techniques, and compared with the Fluke 6105A.

Secondly, a test was performed using an input sinusoidal signal of  $230\text{ V}_{\text{rms}}$  and  $1\text{ A}_{\text{rms}}$ , sweeping its frequency from  $49\text{ Hz}$  to  $51\text{ Hz}$ , with a step of  $0.1\text{ Hz}$ . For each step, 30 repeated measurements were taken; Table 2 shows the percentage maximum relative errors for all measured parameters.

Eventually, several tests have been carried out in order to analyze results of the energy counted by the prototype: the calibrator has a specific feature, which allows supplying a specified amount of energy. Table 3 reports the energy computed by the proposed architecture, with three different value on the Fluke 6105A, (10, 50 and  $100\text{ Wh}$ , with input sinusoidal waveforms of  $230\text{ V}_{\text{rms}}$  and  $1\text{ A}_{\text{rms}}$ ); results are averaged on 30 repeated measurement for each energy value. Furthermore, Table 4 reports the energy computed by the smart power meter in sinusoidal and distorted conditions. Tests are carried out with a waveform of  $230\text{ V}_{\text{rms}}$  and a sinusoidal current of  $4\text{ A}_{\text{rms}}$  at  $50\text{ Hz}$ , and fixing the energy supplied by the calibrator to  $1\text{ kWh}$ . The first row is referred to a sinusoidal input waveform of  $230\text{ V}_{\text{rms}}$ . The second row is referred to a signal at  $50\text{ Hz}$ , with a second harmonic, resulting in a signal with a THD of  $21.7\%$  ( $224.75\text{ V}$  for the fundamental and  $48.86\text{ V}$  for the second harmonic). Whereas the third row is referred to a signal at  $50\text{ Hz}$ , with also a third harmonic, resulting in a signal with a THD of  $31.1\%$  ( $219.62\text{ V}$  for the fundamental,  $47.74\text{ V}$  for the second harmonic, and  $48.86\text{ V}$  for the third harmonic).

Table 2

Percentage Max relative frequency errors for sinusoidal signal, in the range  $49\text{--}51\text{ Hz}$ .

	$V_{\text{rms}}$	$I_{\text{rms}}$	S	P	Q	PF
Maximum relative Error [%]	0.28	0.35	0.62	0.20	0.68	0.01

Table 3

Percentage relative energy errors for sinusoidal signal.

Energy imposed by Fluke [Wh]	10.00	50.00	100.00
Relative error [%]	0.55	0.15	0.11

Table 4

Results in distorted conditions with fixed supplied energy of  $1\text{ kWh}$ .

THD [%]	Mean [Wh]	Stan. dev. [Wh]	Rel. error [%]
0	998.72	0.59	0.12
21.7	998.44	0.34	0.15
31.1	998.38	0.24	0.16

Table 5

Results of energy computed with different frequencies with fixed supplied energy of  $1\text{ kWh}$ .

Input frequency [Hz]	energy measured [Wh]
49.9	998.61
50.0	998.76
50.1	998.87

These are results of 10 repeated measurements for each input signal waveform. In Table 5 results of energy computed by the smart meter proposed with different fixed input frequency are shown: tests are carried out with sinusoidal waveforms of 230 V<sub>rms</sub> and 4 A<sub>rms</sub> at different frequencies and fixing the input the energy supplied by the calibrator at 1 kWh.

Also, the execution time of the implemented algorithm previously described on the proposed smart power meter has been evaluated using a feature of the uVision development tool.

More in details, only 200  $\mu$ s are needed for the computation of both the Goertzel and Fryze algorithms confirming the real-time behavior desired.

## 5. Conclusion

The paper proposes a prototype of a low cost electrical smart power meter which has been designed to be included in an IoT scenario. The wM-Bus radio module used by the smart power meter allows the inclusion of them in a common IoT scenario as the advanced metering infrastructure, already used for the smart metering of water and gas consumption. The radio module could also work as repeater, helping network designers in optimal siting of gateways in urban areas. Thanks to the implemented metrics, the active and non-active power with bi-directional measurement can be made in non-sinusoidal conditions without reducing accuracy. Synchronous sampling must be ensured to minimize the error in the estimation of power. Two algorithms, for the evaluation of the period, with a low computational impact are considered. A comparison between the two algorithms is reported both in simulation and on real signals. The set of tests conducted on this low cost smart power meter highlighted the good performance. The temperature dependence of the measuring module has been considered and minimized. The small computational time required for the execution of the algorithms previously described, allows the real-time execution of the evaluation of the energy delivered, taking into account also the network frequency changes. Future developments will concern the improvement of other power quality metric on board and the evaluation of the smart power meter in a real city IoT scenario.

## References

- [1] K.R. Kunzmann, Smart cities: a new paradigm of urban development, in: Crios, 2014, pp. 1–4. <http://doi.org/10.7373/77140>.
- [2] J. Jin, J. Gubbi, S. Marusic, M. Palaniswami, An information framework for creating a smart city through internet of things, *IEEE Internet Things J.* 1 (2) (2014) 112–121, <https://doi.org/10.1109/JIOT.2013.2296516>.
- [3] A. Zanella, N. Bui, A. Castellani, L. Vangelista, M. Zorzi, Internet of things for smart cities, *IEEE Internet Things J.* 1 (1) (2014) 22–32, <https://doi.org/10.1109/JIOT.2014.2306328>.
- [4] P. Mohanty, U. Choppali, E. Kougianos, Everything you wanted to know about smart cities, *IEEE Consumer Electron. Mag.* 5 (3) (2016) 60–70, <https://doi.org/10.1109/MCE.2016.2556879>.
- [5] I. Shallari, S. Krug, M. O'Nils, Architectural evaluation of node – server partitioning for people counting, in: International Conference on Distributed Smart Cameras, Eindhoven, Netherlands, 2018, <https://doi.org/10.1145/3243394.3243688>.
- [6] G. Di Leo, M. Landi, V. Paciello, A. Pietrosanto, Smart metering for demand side management, in: Proceedings of the IEEE Instrumentation and Measurement Technology Conference I2MTC, 2012, pp. 1798–1803, <https://doi.org/10.1109/I2MTC.2012.6229246>.
- [7] M. Masera, F. Bompard, F. Profumo, N. Hadjsaid, Smart (electricity) grids for smart cities: assessing roles and societal impacts, *Proc. IEEE* 106 (4) (2018) 613–625, <https://doi.org/10.1109/JPROC.2018.2812212>.
- [8] Litos Strategic Communication, The Smart Grid: An Introduction, prepared for the U.S. Department of Energy.
- [9] S. Grijalva, M.U. Tariq, Prosumer-based smart grid architecture enables a flat, sustainable electricity industry, in: Innovative Smart Grid Technologies (ISGT), 2011, pp. 17–19. <http://doi.org/10.1109/ISGT.2011.5759167>.
- [10] Y. Cheng, L. Zhang, Dynamic response model between power demand and power tariff, International Conference on Power System Technology, vol. 2, 2014, pp. 1416–1421. <http://doi.org/10.1109/ICPST.2004.1460224>.
- [11] C. Chen, K.G. Nagananda, G. Xiong, S. Kishore, L.V. Snyder, A communication-based appliance scheduling scheme for consumer-premise energy management systems, *IEEE Trans. Smart Grid* 4 (1) (2013) 56–65, <https://doi.org/10.1109/TSG.2012.2224388>.
- [12] G. Xiong, C. Chen, S. Kishore, A. Yener, Smart (in-home) power scheduling for demand response on the smart grid, in: ISGT, 2011, pp. 1–7. <http://doi.org/10.1109/ISGT.2011.5759154>.
- [13] C. Gungor, D. Sahin, T. Kocak, C. Buccella, C. Cecati, P. Hancke, Smart grid technologies: communication technologies and standards, *IEEE Trans. Ind. Inf.* 7 (4) (2011) 529–539, <https://doi.org/10.1109/TII.2011.2166794>.
- [14] R. Morello, C. Mukhopadhyay, Z. Liu, D. Slomovitz, R. Samantaray, Advances on sensing technologies for smart cities and power grids: a review, *IEEE Sensor J.* 17 (23) (2017) 7596–7610, <https://doi.org/10.1109/JSEN.2017.2735539>.
- [15] R. Morello, C. De Capua, G. Fulco, C. Mukhopadhyay, A Smart power meter to monitor energy flow in smart grids: the role of advanced sensing and IoT in the electric grid of the future, *IEEE Sensor J.* 7 (23) (2017) 7828–7837, <https://doi.org/10.1109/JSEN.2017.2760014>.
- [16] Bo Wang, Dong Liu, Xin Shan, Su Dawei, Qibing Zhang, A detection method for response time of overall primary frequency regulation of power grid, 2017 IEEE Conference on Energy Internet and Energy System Integration (EI2), 2018. <http://doi.org/10.1109/EI2.2017.8245362>.
- [17] Emanuel Serban, Martin Ordóñez, Cosmin Pondiche, Voltage and frequency grid support strategies beyond standards, *IEEE Trans. Power Electron.* 32 (1) (2017) 298–309, <https://doi.org/10.1109/TPEL.2016.2539343>.
- [18] Nilanjan Mukherjee, Dipankar De, Neha Nandagaoli, Effect of sudden variation of grid voltage in primary frequency control application using converter based energy storage systems for weak grid systems, 19th European Conference on Power Electronics and Applications (EPE'17 ECCE), 2017. <http://doi.org/10.23919/EPE17ECCEEurope.2017.8099217>.
- [19] Zhongwei Li, Biying Pei, Xiao Zhang, Huizhong Liu, Weiming Tong, A bidirectional electric energy metering algorithm based on the fundamental component extraction and alternating current sampling, 2nd IEEE Advanced Information Management, Communicative Electronic and Automation Control Conference, 2018. <http://doi.org/10.1109/IMCEC.2018.8469438>.
- [20] K.V. Suslov, V.S. Stepanov, N.N. Solonina, Smart grid: Effect of high harmonics on electricity consumers in distribution networks, *International Symposium on Electromagnetic Compatibility*, 2013, Electronic ISBN: 978-1-4673-4980-2.
- [21] Victor M. Moreno, Alberto Pigazo, Modified FBD method in active power filters to minimize the line current harmonics, *IEEE Trans. Power Delivery* 22 (1) (2007) pp. <https://doi.org/10.1109/TPWRD.2006.886769>.
- [22] V. Paciello, A. Pietrosanto, P. Sommella, Smart sensors for demand response, *IEEE Sens. J.* 17 (23) (2017) 7611–7620, <https://doi.org/10.1109/JSEN.2017.2728611>.
- [23] M. Carratù, M. Ferro, V. Paciello, A. Pietrosanto, P. Sommella, Performance analysis of wM-bus networks for smart metering, *IEEE Sens. J.* 17 (23) (2017) 7849–7856, <https://doi.org/10.1109/JSEN.2017.2738102>.
- [24] F. Abate, M. Carratù, C. Liguori, M. Ferro, V. Paciello, Smart meter for the IoT, in: 2018 IEEE International Instrumentation and Measurement Technology Conference (I2MTC), May 2018, 2018, pp. 889–894. <http://doi.org/10.1109/I2MTC.2018.8409838>.
- [25] M. Carratù, M. Ferro, V. Paciello, A. Pietrosanto, Smart power meter for the IoT, 2018 16th IEEE International Conference on Industrial Informatics, Portugal, 18–20 July, 2018.
- [26] F. Facchini, G.M. Vitetta, A. Losi, F. Ruscelli, On the performance of 169 MHz WM-bus and 868 MHz LoRa technologies in smart metering applications, 2017 IEEE 3rd International Forum on Research and Technologies for Society and Industry (RTSI), 2017. <http://doi.org/10.1109/RTSI.2017.8065900>.
- [27] G. Štruklec, J. Maršić, Implementing DLMS/COSEM in smart meters, in: 2011 8th International Conference on the European Energy Market (EEM), Zagreb, Croatia, 25–27 May, 2011, pp. 747–753.
- [28] L.S. Czarnecki, L.S.C.I. Budeanu, S. Fryze, Two frameworks for interpreting power properties of circuits with nonsinusoidal voltages and currents, *Electr. Eng.* 80 (6) (1997) 359–367, <https://doi.org/10.1007/BF01232925>.
- [29] P. Sysel, P. Rajmic, Goertzel algorithm generalized to non-integer multiples of fundamental frequency, *EURASIP J. Adv. Signal Process.* 56 (2012), <https://doi.org/10.1186/1687-6180-2012-56>.
- [30] A.E. Emanuel, Summary of IEEE Standard 1459: definitions for the measurement of electric power quantities under sinusoidal, nonsinusoidal, balanced, or unbalanced conditions, *IEEE Trans. Ind. Appl.* 40 (3) (2004) 869–876, <https://doi.org/10.1109/TIA.2004.827452>.
- [31] S. Fryze, Active, reactive, and apparent power in non-sinusoidal systems, *Przeglad Elektrot* 7 (1931) 193–203.
- [32] A.V. Oppenheim, R.W. Schaffer, Discrete-Time Signal Processing, 3rd ed. - Pearson New International edition; 2014. ISBN: 9781292038155.
- [33] D.O. Johnson, K.A. Hassani, Issues of power quality in electrical systems, *Int. J. Energy Power Eng.* 5 (4) (2016) 148–154, <https://doi.org/10.11648/j.ijepe.20160504.12>.
- [34] Y.C. Chen, J.K. Lan, Implementation of power measurement system with fourier series and zero-crossing algorithm, in: 2014 International Symposium on Computer, Consumer and Control, June 2003, 2003, pp. 601–604. <http://doi.org/10.1109/IS3C.2014.163>.
- [35] <http://www.st.com/en/DM00037051.pdf>.
- [36] OIML R-46, Active Electrical Energy Meters. Part 1: Metrological and technical requirements. Part 2: Metrological controls and performance tests, Edition 2012 (E).

- [37] H. Serra, J. Correia, A.J. Gano, A.M. de Campos, I. Teixeira, Domestic power consumption measurement and automatic home appliance detection, in: IEEE International Workshop on Intelligent Signal Process, 2005, pp. 128–132. <http://doi.org/10.1109/WISP.2005.1531645>.
- [38] F. Li, P. Xiong, Practical secure communication for integrating wireless sensor networks into the internet of things, IEEE Sens. J. 13 (10) (2013) 3677–3684, <https://doi.org/10.1109/JSEN.2013.2262271>.
- [39] S. Luan, J. Teng, S. Chan, L. Hwang, Development of an automatic reliability calculation system for advanced metering infrastructure, in: in 2010 8th IEEE International Conference on Industrial Informatics, 2010, pp. 342–347. <http://doi.org/10.1109/INDIN.2010.5549395>.
- [40] IEEE – Adoption of IEC 61000, Electromagnetic compatibility (EMC) testing and measurement techniques.